THEORETICAL STUDY OF THE MAGNETIC FIELD IN THE LUNAR WAKE

Y. C. WHANG*

Laboratory for Space Sciences
Goddard Space Flight Center
National Aeronautics and Space Administration
Greenbelt, Maryland

January 1968

ABSTRACT

When the solar wind interacts with the moon, the plasma shadow region on the dark side of the moon forms a long lunar wake. In the plasma umbra a detectable plasma flow is absent; and in the penumbra the plasma flux increases from the void condition in the umbra to the interplanetary condition outside. A theoretical model for perturbations of the magnetic field in the plasma shadow is studied by directly solving Maxwell's equations for steady state solutions. The perturbation of the field is assumed to be due to the magnetization current, the gradient drift current and the curvature drift current. Numerical solutions are obtained to describe the variations of the magnetic field. The results obtained are in good agreement with experimental observations from the Explorer 35 satellite.

I. INTRODUCTION

In a recent paper[1], hereafter to be referred to as Paper 1, the solar wind flow around the moon has been treated as a free molecule flow of guiding-center plasma. Under the assumption that the guiding-center particles move along straight-line paths unless intercepted by the moon's surface, analytical solutions have been obtained to describe the ion flow field in the vicinity of the moon. Theoretical results predict that when the solar wind interacts with the moon, a long non-cylindrically symmetrical lunar wake forms downstream of the moon. The theoretical description of the flow conditions in the interaction region given in Paper 1 agrees very well with experimental observations[2-5] from the lunar orbiting satellite Explorer 35: (1) Shock waves, especially a bow shock, do not exist in the vicinity of the moon, and (2) a plasma shadow region forms on the dark side of the moon. In the umbral region a detectable plasma flow is absent; and in the penumbral region the plasma flux increases from the void condition in the umbra to the interplanetary condition outside.

The magnetic field experiments[2,4,5] on the Explorer 35 spacecraft have revealed many interesting features of the interplanetary magnetic field in the lunar wake. The interplanetary magnetic field appears to be convected through the lunar body without large perturbations. As the satellite passes through the lunar wake, the magnitude of the magnetic field is observed to increase in the umbral region, while outside the umbra the perturbation of the magnetic field appears to follow a coherent pattern of alternating decreases and increases in the magnitude of the field.

Ness et al.[5] suggested that perturbations of the magnetic field in the vicinity of the moon are due to the induced electric current contributed from three sources: the magnetization current, the gradient drift current and the curvature drift current. A theoretical investigation of the perturbations of the magnetic field in the lunar wake due to the induced electric current is reported in this paper.

A steady state solution is studied assuming that upstream of the moon the undisturbed interplanetary magnetic field $\underset{\sim}{B}_o$ is not aligned with the direction of the undisturbed solar wind velocity $\underset{\sim}{U}_o$[6,7]. In Paper 1, the flow field has been found to be symmetrical about the plane passing through the center of the moon and parallel to both $\underset{\sim}{U}_o$ and $\underset{\sim}{B}_o$. Variations of the magnetic field in the plane of symmetry are calculated by considering that the number density N and the parallel pressure $P_{\parallel}$ of the plasma are approximated by the free molecule flow solution, the so called "zeroth order" solution, obtained in Paper 1. Theoretical solutions obtained under this approximation can explain the gross features of the perturbations of the interplanetary magnetic field observed in the lunar wake.

Inevitably, perturbations of the magnetic field and the induced electric field will slightly modify the trajectory of the guiding-center particle and hence modify the plasma flow. This modification should produce a "first order" theoretical solution for the plasma flow. Of course this first order solution will in turn modify the solution for the field perturbations. These higher order effects are not included in the present study.

II. GOVERNING EQUATIONS

The variation of the magnetic field is governed by Maxwell's equations. Under the assumption that the density of the total electric current in the lunar wake is composed of the density of the magnetization current, $\underset{\sim}{J}_M$, the gradient drift current, $\underset{\sim}{J}_G$, and the curvature drift current, $\underset{\sim}{J}_R$, Maxwell's equations can be written as

$$\underset{\sim}{\nabla} \cdot \underset{\sim}{B} = 0 \tag{1}$$

and

$$\underset{\sim}{\nabla} \times \underset{\sim}{B} = \frac{4\pi}{c} (\underset{\sim}{J}_M + \underset{\sim}{J}_G + \underset{\sim}{J}_R). \tag{2}$$

Let $\underset{\sim}{C}$ denote the relative velocity of a charged particle with respect to the moving magnetic line, and $\underset{\sim}{e}_1$ the unit vector along the direction of $\underset{\sim}{B}$. The gyration of a charged particle of mass m about the field line with the perpendicular velocity component $\underset{\sim}{C}_\perp$ gives rise to a magnetic moment

$$\underset{\sim}{\mu} = - \frac{m C_\perp^2}{2 B} \underset{\sim}{e}_1.$$

The magnetic moment is related to the perpendicular pressure, $P_\perp$, by

$$P_\perp = B \int \mu f d\underset{\sim}{C}$$

where f is the distribution function. Thus the adiabatic invariant of the magnetic moment is equivalent to

$$P_\perp / N B = \text{constant}, \tag{3}$$

where N denotes the number density of the charged particles. Other approaches to yield Eq. (3) can be found in References 8 and 9. The density of the magnetization current can be expressed as

$$\underset{\sim}{J}_M = - \underset{\sim}{\nabla} \times (\underset{\sim}{e}_1 \; P_\perp \; c/B). \tag{4}$$

In the presence of a gradient of the magnetic field or a curvature of the field line, the gradient and the curvature drift velocity of a particle of charge q are respectively

$$\underset{\sim}{u}_G = (\mu c/q\, B)\; \underset{\sim}{e}_1 \times \underset{\sim}{\nabla} B$$

$$\underset{\sim}{u}_R = (m C_\parallel^2 c/qB) \underset{\sim}{e}_1 \times (\underset{\sim}{e}_1 \cdot \underset{\sim}{\nabla}\; \underset{\sim}{e}_1).$$

Since particles of opposite charge will drift in opposite directions, electric currents are produced by the gradient and the curvature drift. The parallel velocity of particles with respect to the moving magnetic line is related to the parallel pressure by

$$P_\parallel = \int m\, C_\parallel^2 f \; d\, \underset{\sim}{C} \; .$$

Thus the density of the gradient drift current and of the curvature drift current can be expressed as

$$\underset{\sim}{J}_G = (P_\perp c/B^2) \underset{\sim}{e}_1 \times \underset{\sim}{\nabla} B \tag{5}$$

and

$$\underset{\sim}{J}_R = (P_\parallel c/B) \underset{\sim}{e}_1 \times (\underset{\sim}{e}_1 \cdot \underset{\sim}{\nabla} \underset{\sim}{e}_1). \tag{6}$$

Making use of equations (3)-(6), Eq. (2) can be expressed as

$$(1+\frac{4\pi P_\perp}{B^2})\nabla\times\underset{\sim}{B} = \frac{4\pi}{B}\,\underset{\sim}{e}_1 \times(\frac{P_\perp}{N}\,\nabla N + P_\parallel \underset{\sim}{e}_1\cdot\nabla\underset{\sim}{e}_1) \tag{7}$$

Here the last term on the right hand side is due to the curvature drift current.

Let the subscript $_o$ denote the undisturbed interplanetary condition upstream of the moon. Then in terms of the following dimensionless variables:

$$\underset{\sim}{b} = \underset{\sim}{B}/B_o, \quad n = N/N_o, \quad p = P_\parallel/P_{\parallel o},$$

and the dimensionless parameters:

$$\beta = 8\pi\, P_{\perp o}/B_o^{\,2}, \quad \eta = P_{\parallel o}/P_{\perp o},$$

Maxwell's equations [(1) and (7)] can be reduced to the following dimensionless form,

$$\nabla\cdot\,\underset{\sim}{b} = o \tag{8}$$

and

$$(n+\frac{2b}{\beta})\,\nabla\times\underset{\sim}{b} = \underset{\sim}{b}\times\nabla n + \eta p\,\underset{\sim}{e}_1\times(\underset{\sim}{e}_1\cdot\nabla\underset{\sim}{e}_1). \tag{9}$$

Let $\underset{\sim}{e}_2$ and $\underset{\sim}{e}_3$ be respectively the normal and binormal vector to the line of force. Then using the Serret-Frenet formulas, it can be shown that

$$\nabla\times\underset{\sim}{b} = b\Omega\underset{\sim}{e}_1 + \frac{\partial\, b}{\partial x_3}\,\underset{\sim}{e}_2 + (b\varkappa - \frac{\partial\, b}{\partial \mathbf{x}_2})\underset{\sim}{e}_3$$

and

$$\underset{\sim}{b} \times \nabla n + \eta p \underset{\sim}{e_1} \times (\underset{\sim}{e_1} \cdot \nabla \underset{\sim}{e_1}) = \underset{\sim}{e_2} \left(-b \frac{\partial n}{\partial x_3}\right) + \underset{\sim}{e_3} \left(b \frac{\partial n}{\partial x_2} + \eta p \kappa\right).$$

Here κ is curvature of the field-lines and $\Omega \equiv \frac{\partial \underset{\sim}{e_1}}{\partial x_2} \cdot \underset{\sim}{e_3} - \frac{\partial \underset{\sim}{e_1}}{\partial x_3} \cdot \underset{\sim}{e_2}$ is called the abnormality of the field. Making use of these two equations, (9) may be resolved along the directions $\underset{\sim}{e_1}$, $\underset{\sim}{e_2}$ and $\underset{\sim}{e_3}$ to give

$$\left.\begin{aligned} \Omega &= 0 \\ \left(n + \frac{2b}{\beta}\right) \frac{\partial b}{\partial x_3} &= - b \frac{\partial n}{\partial x_3} \end{aligned}\right\} \quad (10)$$

and $$\left(n + \frac{2b}{\beta}\right) \frac{\partial b}{\partial x_2} = - b \frac{\partial n}{\partial x_2} + \kappa \left[\left(n + \frac{2b}{\beta}\right) b - \eta p\right].$$

Eqs. (10) indicate that (i) abnormality of the field is always zero which means there is no torsion of neighboring field-lines, and (ii) the curvature drift current ($\eta p \kappa \underset{\sim}{e_3}$) does not directly effect the variation of $\underset{\sim}{b}$ along the binormal direction.

III PLANE OF ANALYSIS

Cylindrical coordinates (r, θ, Z) will be used in this paper to study the equations formulated in Section II. The origin of the coordinates is located at the moon's center, and the Z-axis is perpendicular to both the undisturbed solar wind velocity $\underset{\sim}{U}_o$ with respect to the center of the moon and the undisturbed interplanetary magnetic field $\underset{\sim}{B}_o$ upstream of the moon. The scale of the coordinate system is normalized by using the moon's radius as a unit length.

The distribution of the plasma density and the distribution of the magnetic field are symmetrical about Z = 0 plane. On the plane of symmetry

$$b_z = \frac{\partial b}{\partial x_3} = \frac{\partial n}{\partial x_3} = 0.$$

It can be seen from (10) that Eq. (9) has only one non-zero component along the binormal direction (Z-direction). Thus the variation of the magnetic field on the plane of symmetry (Z = 0 plane) is governed by two equations

$$\frac{1}{r}\frac{\partial}{\partial r}(r\, b_r) + \frac{1}{r}\frac{\partial b_\theta}{\partial \theta} + \frac{\partial b_z}{\partial Z} = 0 \qquad (11)$$

and

$$\left(n + \frac{2b}{\beta}\right)\left[\frac{1}{r}\frac{\partial}{\partial r}(r b_\theta) - \frac{1}{r}\frac{\partial b_r}{\partial \theta}\right]$$

$$= \frac{b_r}{r}\frac{\partial n}{\partial \theta} - b_\theta \frac{\partial n}{\partial \theta} + \gamma\beta\left[\frac{\sin\Psi}{r}\left(1 + \frac{\partial \Psi}{\partial \theta}\right) + \cos\Psi\frac{\partial \Psi}{\partial r}\right] \qquad (12)$$

where $\Psi \equiv \arctan (b_\theta / b_r)$. Through the third term on the left hand side of (11), the variation of magnetic field on the plane of symmetry couples with the field on its neighboring planes. In the neighborhood of the Z = 0 plane, the field lines are essentially parallel to this plane. The third term in Eq. (11) is in general small compared with the other two terms. In order to analyze the variation of $\underset{\sim}{b}$ on the plane of symmetry, it is assumed that on this plane of analysis the term $\partial b_z / \partial Z$ can be neglected from (11), thus yielding

$$\frac{\partial}{\partial r} (r b_r) + \frac{\partial b_\theta}{\partial \theta} = 0. \tag{13}$$

Eqs. (12) and (13) suffice to solve for the two unknowns b_r and b_θ on the plane of analysis provided that n and p are known functions of r and θ.

Introducing a new function A, such that

$$\left.\begin{aligned} b_r &= \frac{1}{r} \frac{\partial A}{\partial \theta} \\ \text{and} \qquad b_\theta &= - \frac{\partial A}{\partial r} , \end{aligned}\right\} \tag{14}$$

Eq. (13) is satisfied. Eq. (12) can now be written as

$$\begin{aligned} &\frac{1}{r} \frac{\partial}{\partial r} \left(r \frac{\partial A}{\partial r}\right) + \frac{1}{r^2} \frac{\partial^2 A}{\partial \theta^2} \\ &= - \left(n + \frac{2b}{\beta}\right)^{-1} \left\{ \frac{\partial n}{\partial r} \frac{\partial A}{\partial r} + \frac{1}{r^2} \frac{\partial n}{\partial \theta} \frac{\partial A}{\partial \theta} + \eta p \left[\frac{\sin \Psi}{r} \left(1 + \frac{\partial \Psi}{\partial \theta}\right) + \cos \Psi \frac{\partial \Psi}{\partial r} \right] \right\} \end{aligned} \tag{15}$$

If the plasma density were not perturbed in the vicinity of the moon (i.e. n = 1 everywhere), then the trivial solution of (15) would represent the undisturbed field with

$$A_o = r \cos (\phi_o - \theta) \tag{16}$$

where ϕ_o is the direction angle of the undisturbed magnetic field, that is the angle between $-\underset{\sim}{U}_o$ and $\underset{\sim}{B}_o$. The zeroth order solutions for N/N_o and $P_\perp/P_{\parallel o}$ calculated from a free molecule flow model in Paper 1 will be substituted into Eq. (15) to calculate A. The maximum perturbation of b by the lunar wake is of the order of 30 percent. The effect of the field perturbation and the induced electric field on N/N_o and $P_\parallel/P_{\parallel o}$ is not included in the calculation. The zeroth order solution of N/N_o and $P_\parallel/P_{\parallel o}$ are known functions of position and two dimensionless parameters: the direction angle ϕ_o and the speed ratio S:

$$S = U_o/(2kT_{\parallel o}/m_i)^{\frac{1}{2}},$$

where the parallel temperature of the plasma $T_\parallel$ is defined as

$$kT_\parallel/2 = (1/N) \int_{-\infty}^{\infty} (mC_\parallel^2/2) f d\underset{\sim}{C}.$$

Therefore, the solution of Eq. (15) will depend on four dimensionless parameters: $\parallel$, S, ϕ_o, and β.

Eq. (15) will be studied in a closed region between two concentric circles: $1 \leq r \leq R$. If the outer boundary r=R is chosen at a distance very far away from the lunar surface, i.e., $R \gg 1$, then it may be assumed that the field is not disturbed on the boundary r=R. It is also assumed that

the field lines are smoothly convected through the lunar body so that the field is not disturbed in its interior or on the lunar surface. Thus the boundary conditions of the problem can be written as

$$\left.\begin{aligned} &A(r=1,\ \theta) = \cos(\phi_o - \theta), \\ \text{and}\quad &A(r=R,\ \theta) = R\cos(\phi_o - \theta). \end{aligned}\right\} \quad (17)$$

A rather simple boundary condition on the lunar surface is assumed in the present study. However, the method of solution developed in this paper can be used to study the same problem once the physical properties of the moon become better understood and a more accurate condition can be prescribed on the lunar body. The effect of the prescribed surface condition on the perturbations of the magnetic field is limited to the immediate neighborhood of the moon, say $r < 2$. In the outside region the perturbations of the magnetic field are dominated by the plasma flow field.

An iterative method is used to find the solution of the nonlinear Poisson equation (15). For this purpose, Eq. (15) may be written as

$$\frac{1}{r}\frac{\partial}{\partial r}\left(r\frac{\partial A_i}{\partial r}\right) + \frac{1}{r^2}\frac{\partial^2 A_i}{\partial \theta^2} = G_{i-1} \quad (i = 1,2,\cdots) \qquad (18)$$

where

$$G_{i-1} = -\left(n + \frac{2}{\beta}\, b_{i-1}\right)^{-1} \left\{\frac{\partial n}{\partial r}\frac{\partial A_{i-1}}{\partial r} + \frac{1}{r^2}\frac{\partial n}{\partial \theta}\frac{\partial A_{i-1}}{\partial \theta} + \eta p\left[\frac{\sin\Psi_{i-1}}{r}\cdot\left(1 + \frac{\partial \Psi_{i-1}}{\partial \theta}\right) + \cos\Psi_{i-1}\frac{\partial \Psi_{i-1}}{\partial r}\right]\right\}.$$

At the ith step, G_{i-1} is evaluated based on the solution of A_{i-1}. At the first step, the undisturbed solution (16) is used to evaluate G_o.

In each iteration the source term G_{i-1} is a known function of r and θ, and the numerical problem is to solve Poisson's equation for A_i. For the computations carried out in this paper, the iteration process continues until the condition of convergence

$$|b_i - b_{i-1}| < 0.001$$

is met everywhere in the domain of the solution.

IV. METHOD OF NUMERICAL SOLUTION

The problem to be discussed is the numerical solution of Poisson's equation,

$$\frac{1}{r}\frac{\partial}{\partial r}\left(r\frac{\partial A}{\partial r}\right) + \frac{1}{r^2}\frac{\partial^2 A}{\partial \theta^2} = G(r,\theta) \tag{19}$$

subject to the boundary condition (17). Here the subscripts i and i-1 have been dropped from (18). Recently Hockney[10] has developed a direct method for finding the solution of the Poisson's equation in a rectangular region. His method is extended here to solving Poisson's equation (19) in a region between two concentric circles.

Introducing $s = \ln r$ and $H = r^2 G$, Eq. (19) can be written as

$$\frac{\partial^2 A}{\partial s^2} + \frac{\partial^2 A}{\partial \theta^2} = H \tag{20}$$

The outer boundary is chosen at $R = \exp(6.4) \simeq 600$, where the perturbation of the plasma density is less than two percent. The problem is then to solve Poisson's equation (20) in a closed rectangular region: $0 \le s \le 6.4$ and $0 \le \theta \le 2\pi$ in s,θ-coordinates. The boundary conditions are transformed by the mapping to

$$\left.\begin{aligned} A\ (s=0,\ \theta) &= \cos\ (\phi_o - \theta) \\ A\ (s=6.4,\ \theta) &= \exp\ (6.4)\ \cos\ (\phi_o - \theta) \end{aligned}\right\} \tag{21}$$

and $\qquad A\ (s,\ \theta=0) = A\ (s,\ \theta=2\pi)$

The third boundary condition allows $A(s,\theta)$ to be Fourier analyzed with respect to the azimuthal variable θ,

$$A\ (s,\theta) = \tfrac{1}{2}\ a_c(s,o) + \sum_{n=1}^{N} [a_c(s,n)\ \cos\ n\theta + a_s(s,n)\ \sin\ n\theta] \tag{22}$$

and similarly for $H(s,\theta)$ where $a_c(s,n)$ and $a_s(s,n)$ are the Fourier

amplitudes of the cosine and sine of the nth harmonic. The potential A will be approximated by the first N modes. Computations are carried out in this paper by choosing N=20.

On substituting (22) into (20), the partial differential equation is reduced to two sets of independent ordinary differential equations relating the Fourier amplitudes of $A(s,\theta)$ and $H(s,\theta)$,

$$\left.\begin{aligned} &\frac{d^2}{ds^2} a_c(s,n) - n^2 a_c(s,n) = h_c(s,n) \quad (n=0,1,\ldots,N) \\ \text{and} \quad &\\ &\frac{d^2}{ds^2} a_s(s,n) - n^2 a_s(s,n) = h_s(s,n) \quad (n=1,2,\ldots,N), \end{aligned}\right\} \quad (23)$$

subject to the boundary conditions that at s=0 and s= 6.4,

$$\left.\begin{aligned} &a_c(s,1) = \exp(s)\,\sin\phi_o \\ &a_s(s,1) = -\exp(s)\,\cos\phi_o \\ &a_c(s,n\neq 1) = 0 \\ \text{and} \quad &a_s(s,n\neq 1) = 0. \end{aligned}\right\} \quad (24)$$

Since H is a known function of s and θ, the term on the right-hand side of (23) can be calculated from

$$h_c(s,n) = \frac{1}{\pi}\int_{-\pi}^{\pi} H(s,\theta)\cos n\theta\, d\theta,$$

and

$$h_s(s,n) = \frac{1}{\pi}\int_{-\pi}^{\pi} H(s,\theta)\sin n\theta\, d\theta.$$

The domain of the solution in the s, θ-coordinate is spanned by a (128x360) mesh of uniform mesh spacing

$$\Delta s = 0.05$$

and

$$\Delta\theta = 1 \text{ degree},$$

with $s = 0.05\ m$ $(m = 0,1,2,\ldots\ 128)$

and $\theta = \ell/180$ $(\ell = 0,\ 1,2,\ldots\ 360)$,

where ℓ and m are the indices in the θ and s directions respectively.

The ordinary differential equations (22) may be written in finite difference form as

$$a_{m-1} + f_o a_m + a_{m+1} = g_{o,m} \quad (m=1,2,\ldots,127) \tag{25}$$

where $f_o = -2 - n^2(\Delta s)^2$

and $g_{o,m} = (\Delta s)^2 h_m$.

Here the subscripts s, c and n have been dropped for brevity. a_m has the prescribed values at m=0,128 given in (24). Eq. (25) constitutes a set of 127 algebraic equations for the same number of unknowns a_m (m=1,2,...127), and the numerical problem now is that of determining the a_m's.

The solution of (25) for a_m can be calculated by the technique of recursive cyclic reduction[10]. Consider three neighboring equations from (25)

$$\left.\begin{aligned} a_{m-2} + f_o\, a_{m-1} + a_m &= g_{o,m-1} \\ a_{m-1} + f_o\, a_m + a_{m+1} &= g_{o,m} \\ a_m + f_o\, a_{m+1} + a_{m+2} &= g_{o,m+1} \end{aligned}\right\} \tag{26}$$

for m=2, 4, 6, ...126. By multiplying the second equation by $-f_o$ and adding, one can obtain

$$a_{m-2} + f_1\, a_m + a_{m+2} = g_{1,m} \tag{27}$$

where $f_1 = 2 - f_o^2$

and $g_{1,m} = g_{o,m-1} - f_o\, g_{o,m} + g_{o,m+1}$.

Eq. (27) is identical in form to Eq. (25) except that f_o is replaced by f_1 and $g_{o,m}$ by $g_{1,m}$. While Eq. (25) represents a set of 127 equations, and Eq. (27) represents only 63 equations. This process of reducing the number of equations may be repeated, leading to

$$a_{m-j} + f_k\, a_m + a_{m+j} = g_{k,m} \qquad (k=1,2,\ldots,6) \qquad (28)$$

where $j = 2^k$

$$f_k = 2 - f_{k-1}^2$$

and $$g_{k,m} = g_{k-1,\, m-j/2} - f_{k-1}\, g_{k-1,m} + g_{k-1,\, m+j/2}$$

for m=j, step 2j, until (128-j). For k=6, Eq. (28) gives

$$a_o + f_6\, a_{64} + a_{128} = g_{6,64}.$$

This equation is solved directly for a_{64}. Then from (28), all other intermediate values of a_m are calculated recursively

$$a_m = (g_{k,m} - a_{m-j} - a_{m+j})/f_k.$$

a_{32}, a_{96} are calculated at k=5, a_{16}, a_{48}, a_{80}, a_{112} at k=4, etc.

Having obtained all harmonic amplitudes a_c (s,n) and a_s (s,n) for s=0.05m (m=0, 1, 2, ... 128), the potential A can be calculated at all the nodes of the (128x360) mesh by the process of Fourier synthesis from Eq. (22).

V. RESULTS

For typical interplanetary conditions [7, 11, 12] at the earth's orbit, the magnetic field has a direction angle $\phi_o \sim 135^\circ$ or 315° and the ratio of $P_{\parallel o}$ to $P_{\perp o}$, η, varies between 1.5 and 4 for the solar wind plasma. The speed ratio, S, is of the order of 10, and the β value is of the order of unity. Based on these values, some numerical solutions have been carried out to describe the variations of the magnetic field on the plane of analysis.

Figs. 1 and 2 show the perturbation of the field magnitude, B/B_o, the direction angle, ϕ (defined as the angle between $-\underset{\sim}{U}_o$ and the local field $\underset{\sim}{B}$), and the lines of force in the vicinity of the moon for η=2, S=10, ϕ_o=135° and β=1. The perturbations of the field exhibit a very complex nature. However it can be seen that in the plasma umbral region, the magnitude of the calculated magnetic field, B/B_o, increases to about 25% above the undisturbed condition. On either side of the plasma umbra the magnitude of the field decreases to about 5% below the interplanetary condition. As the magnitude of the field increases in the plasma umbral region, the spacing between lines of force becomes narrower; this causes the direction angle ϕ to increase in the umbral region.

The division of the plasma shadow into umbral and penumbral regions was discussed in Reference 5. Since the plasma density varies continuously through the penumral region from the interplanetary condition N_o to the void condition, it has been suggested[5] that the plasma penumbra be defined as the region where $0.01 < N/N_o < 0.99$ and the plasma umbra, the region with $N/N_o < 0.01$. Follcwing this definition, the distribution of the

lines of force in the two regions is shown in Fig. 3.

The detailed variations of the field magnitude are plotted in Fig. 4, from which the alternating increases and decreases in the magnitude of the magnetic field outside the umbra are noticeable. Solutions for two different speed ratios (S=5 and 10) are plotted in Fig. 4. The solution for S=10 shows a more prominent oscillating pattern of the field magnitude than the solution for S=5. These figures can show the perturbations of the field in the far wake region as well as in the near wake region. As the distance from the moon increases, the anomaly of the magnetic field decreases in magnitude and spreads over a wider region. Comparing the two cases in Fig. 4, it can also be seen that the anomaly of the magnetic field does not seem to be strongly affected by the speed ratio S.

The maximum increases in the magnitude of the field at varying distances r are presented in Fig. 5. It can be seen that for the same values of the direction angle ϕ_o, the maximum anomalies vary only slightly for different speed ratios. However if the speed ratio is held constant, the maximum anomalies vary noticeably with the varying direction angle ϕ_o. This effect may be explained from Eq. (10) as follows. When $\underset{\sim}{B}_o$ is nearly perpendicular to $\underset{\sim}{U}_o$, the gradient of n along the normal direction ($\partial n/\partial x_2$) is relatively small. When the acute angle between $\underset{\sim}{B}_o$ and $\underset{\sim}{U}_o$ decreases, $\partial n/\partial x_2$ increases, and so does the total induced current in the wake region. The increasing source term directly intensifies the anomaly of the magnetic field.

VI. SUMMARY

A theoretical model for variations of the magnetic field in the lunar wake is studied by directly solving Maxwell's equations for steady state solutions. It is assumed that the total electric current is composed of the magnetization current, the gradient drift current and the curvature drift current. The plasma flow in the lunar wake is approximated by the analytical solution obtained from a free molecule flow model[1]. Numerical solutions are obtained to describe the magnetic field in the plane passing through the center of the moon and parallel to both the solar wind velocity and the interplanetary magnetic field upstream of the moon.

As the satellite passes through the solar plasma shadow of the moon, the magnitude of the magnetic field is observed to increase in the umbral region, while outside the umbra the perturbation of the field appears to follow a pattern of alternating decreases and increases in the magnitude of the field. The umbral increases in the magnitude of the magnetic field calculated from this model agree well with experimental observations. The magnitude of the innermost penumbral decreases calculated from this model is too small by a factor of two or more compared with experimental observations. The calculated anomalies of the field oscillations outside the plasma umbra are also smaller than the observed anomalies.

ACKNOWLEDGMENTS

The author is indebted to Drs. Norman F. Ness and Harold E. Taylor for many valuable discussions in the course of this investigation. Also, he wishes to thank Mr. Kenneth W. Behannon for a number of helpful comments.

REFERENCES AND FOOTNOTES

* National Academy of Sciences - National Research Council Senior Postdoctoral Research Associate, on leave from the Catholic University of America.

1. Y. C. Whang, Phys. Fluids 11, (May, 1968).
2. N. F. Ness, K. W. Behannon, C. S. Scearce, and S. C. Canterano, J. Geophys. Res. 72, 5769 (1967).
3. E. F. Lyon, H. S. Bridge, and J. H. Binsack, J. Geophys. Res. 72, 6113 (1967).
4. D. S. Colburn, R. G. Currie, J. D. Mihalov, and C. P. Sonett, Science 158, 1040 (1967).
5. N. F. Ness, K. W. Behannon, H. E. Taylor, and Y. C. Whang, J. Geophys. Res. 73, (1968).
6. E. N. Parker, Astrophys. J. 128, 664 (1958).
7. N. F. Ness, in Annals of the IQSY, A. C. Stickland, Ed., (To be published in 1968).
8. H. Grad, in Electromagnetics and Fluid Dynamics of Gaseous Plasma, J. Fox, Ed., (Polytechnic Press, New York, 1961), pp. 37, 64.
9. C. F. Chew, M. L. Goldberger, and F. E. Low, Proc. Royal Soc. A236, 112 (1956).
10. R. W. Hockney, J. Assoc. Computing Mach. 12, 95 (1965).
11. M. Neugebauer and C. W. Snyder, J. Geophys. Res. 71, 4469 (1966).
12. A. J. Hundhausen, S. J. Bame, and N. F. Ness, J. Geophys. Res. 72, 5265 (1967).

FIGURE CAPTIONS

Figure 1 Distributions of the magnitude of the magnetic field and the lines of force in the vicinity of the moon.

Figure 2 Distributions of the direction angle and the lines of force in the vicinity of the moon.

Figure 3 Distributions of the lines of force in the plasma umbral and the plasma penumbral region.

Figure 4 Variations of the field magnitude for two speed ratios S=5 and S=10.

Figure 5 The maximum increases in the magnitude of the magnitude field at varying distances r.

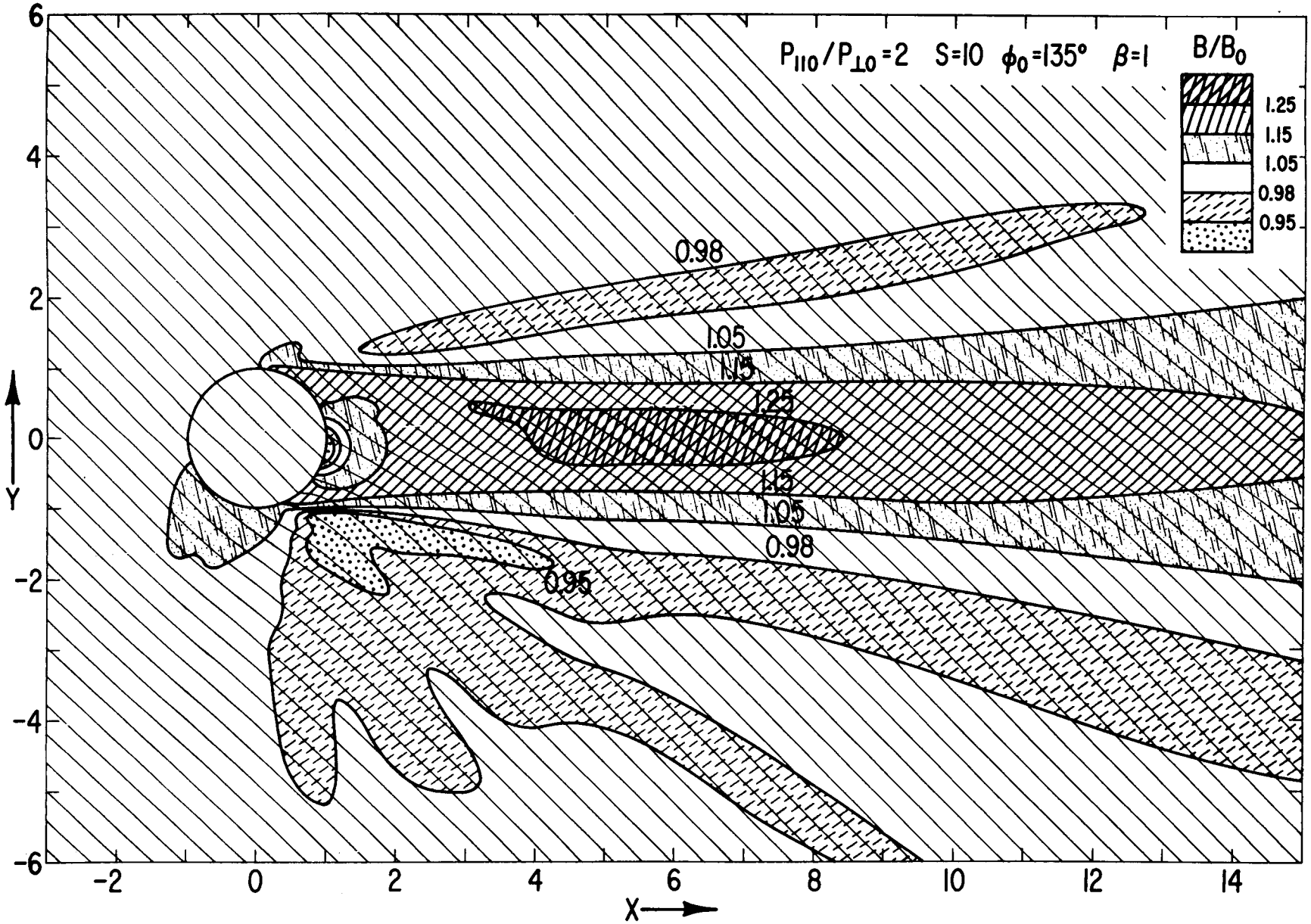
$P_{\parallel 0}/P_{\perp 0}=2$ S=10 $\phi_0=135°$ $\beta=1$
B/B_0
1.25
1.15
1.05
0.98
0.95
0.98
1.05
1.15
1.25
1.15
1.05
0.98
0.95
Y
X
6
4
2
0
-2
-4
-6
-2
0
2
4
6
8
10
12
14

FIG. 1

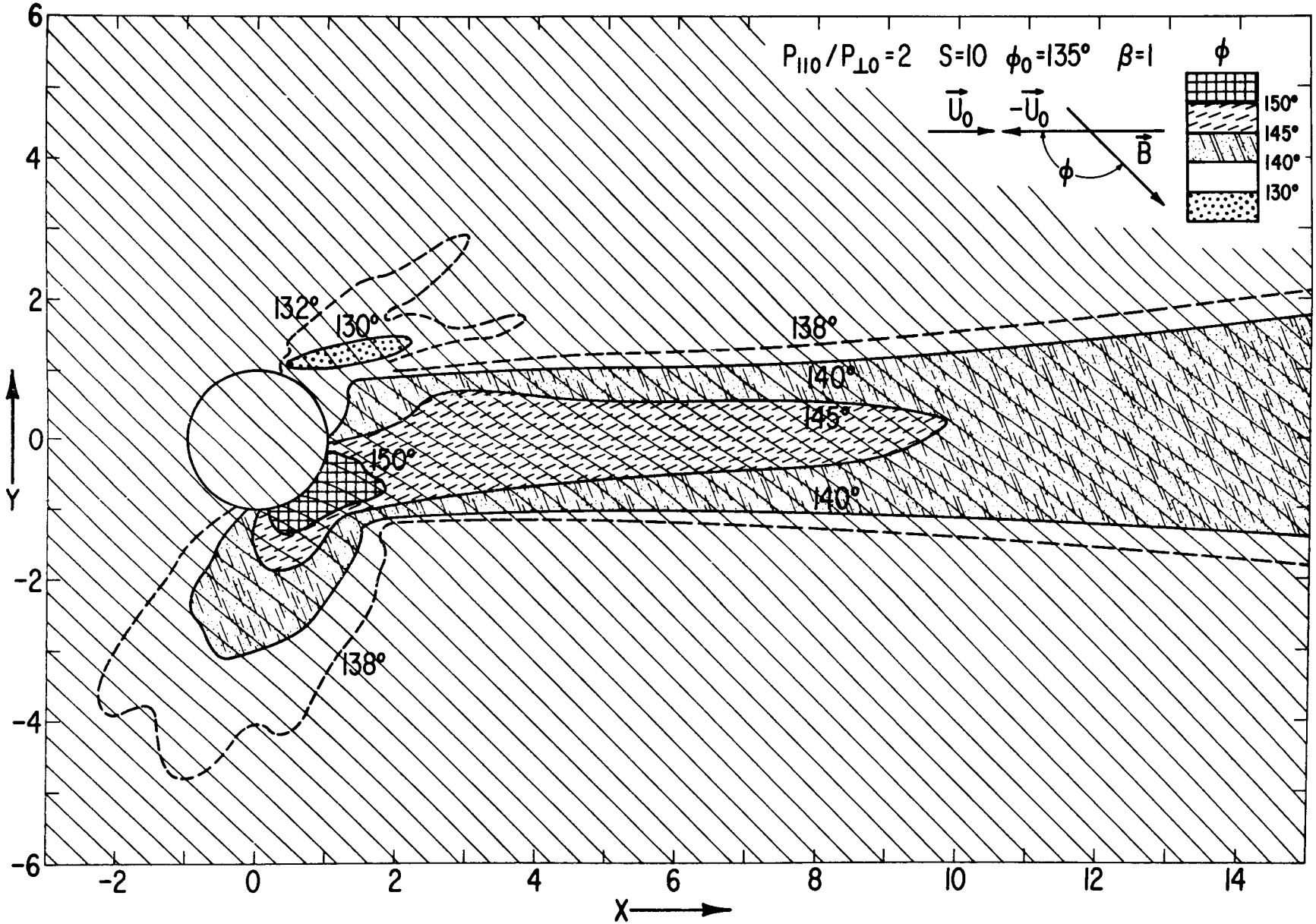
$P_{110}/P_{\perp 0}=2$ S=10 $\phi_0=135°$ $\beta=1$
ϕ
150°
145°
140°
130°
$\vec{U}_0$
$-\vec{U}_0$
$\vec{B}$
ϕ
132°
130°
138°
140°
145°
150°
140°
138°
Y
X
6
4
2
0
-2
-4
-6
-2
0
2
4
6
8
10
12
14

FIG. 2

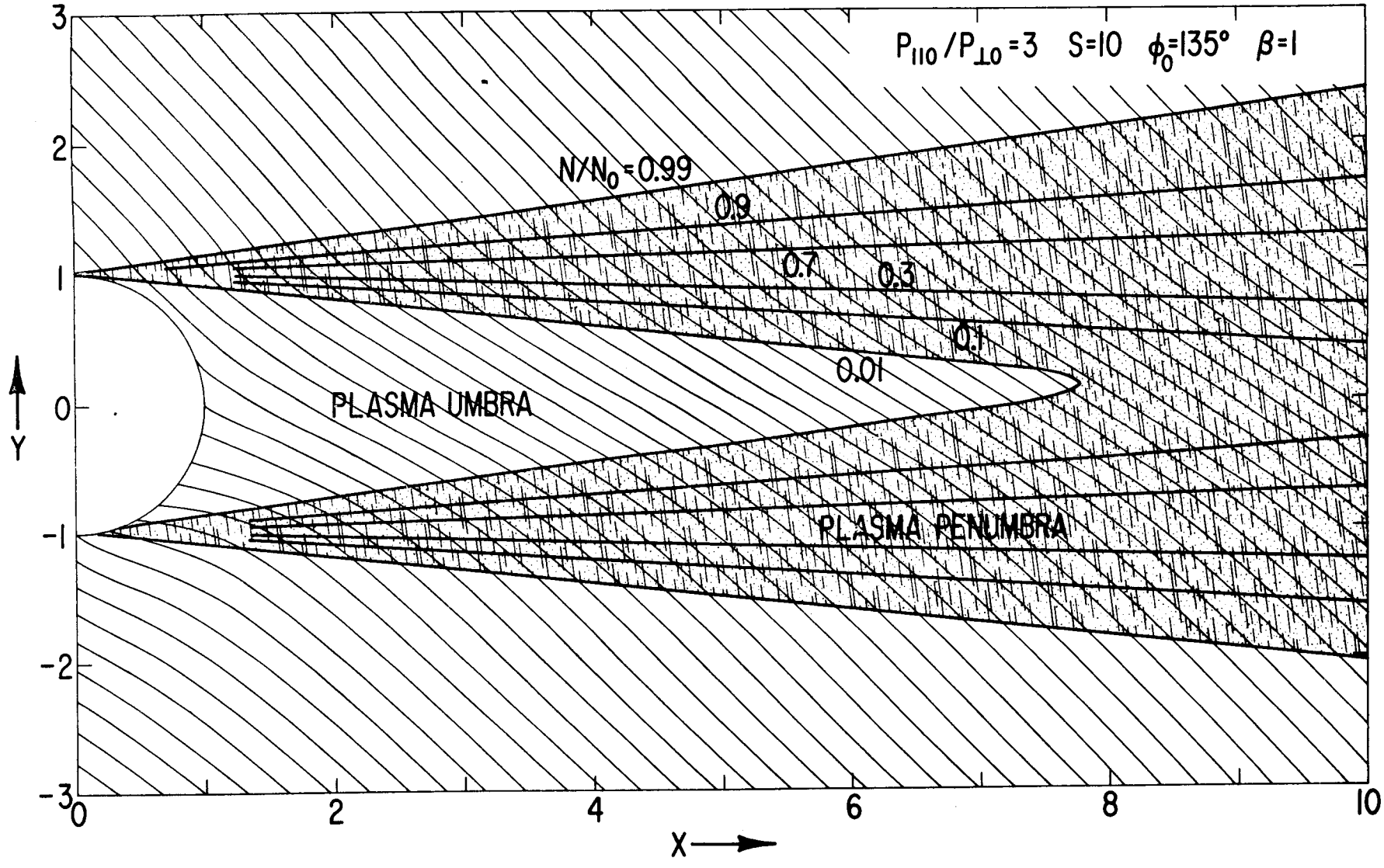
$P_{110}/P_{\perp 0}=3$ S=10 $\phi_0=135°$ $\beta=1$
$N/N_0=0.99$
0.9
0.7
0.3
0.1
0.01
PLASMA UMBRA
PLASMA PENUMBRA
Y
X
3
2
1
0
-1
-2
-3
0
2
4
6
8
10

FIG. 3

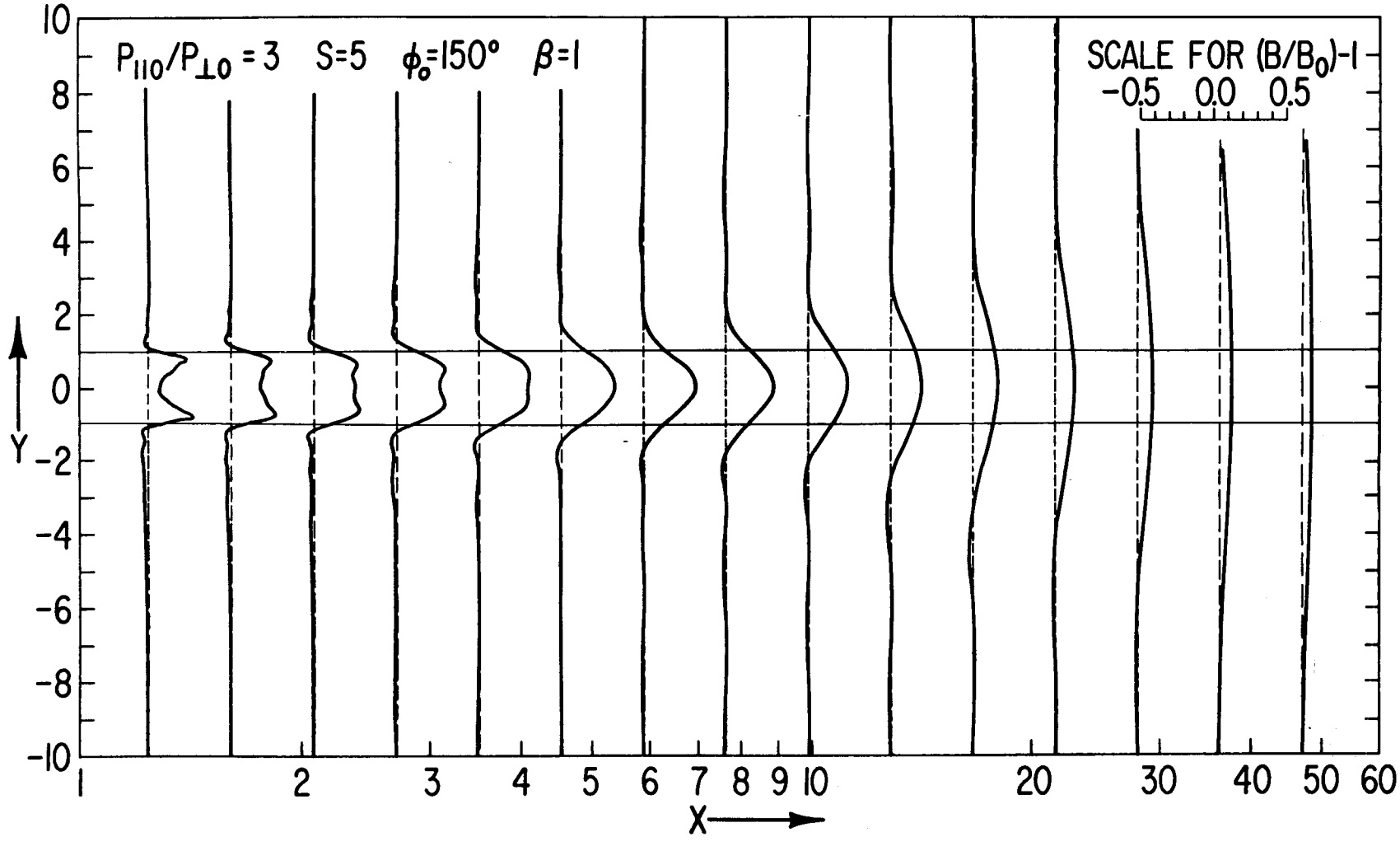
$P_{110}/P_{\perp 0} = 3$ S=5 ϕ_0=150° β=1
SCALE FOR $(B/B_0)-1$
-0.5 0.0 0.5
10
8
6
4
2
0
-2
-4
-6
-8
-10
Y
1 2 3 4 5 6 7 8 9 10 20 30 40 50 60
X

FIG. 4A

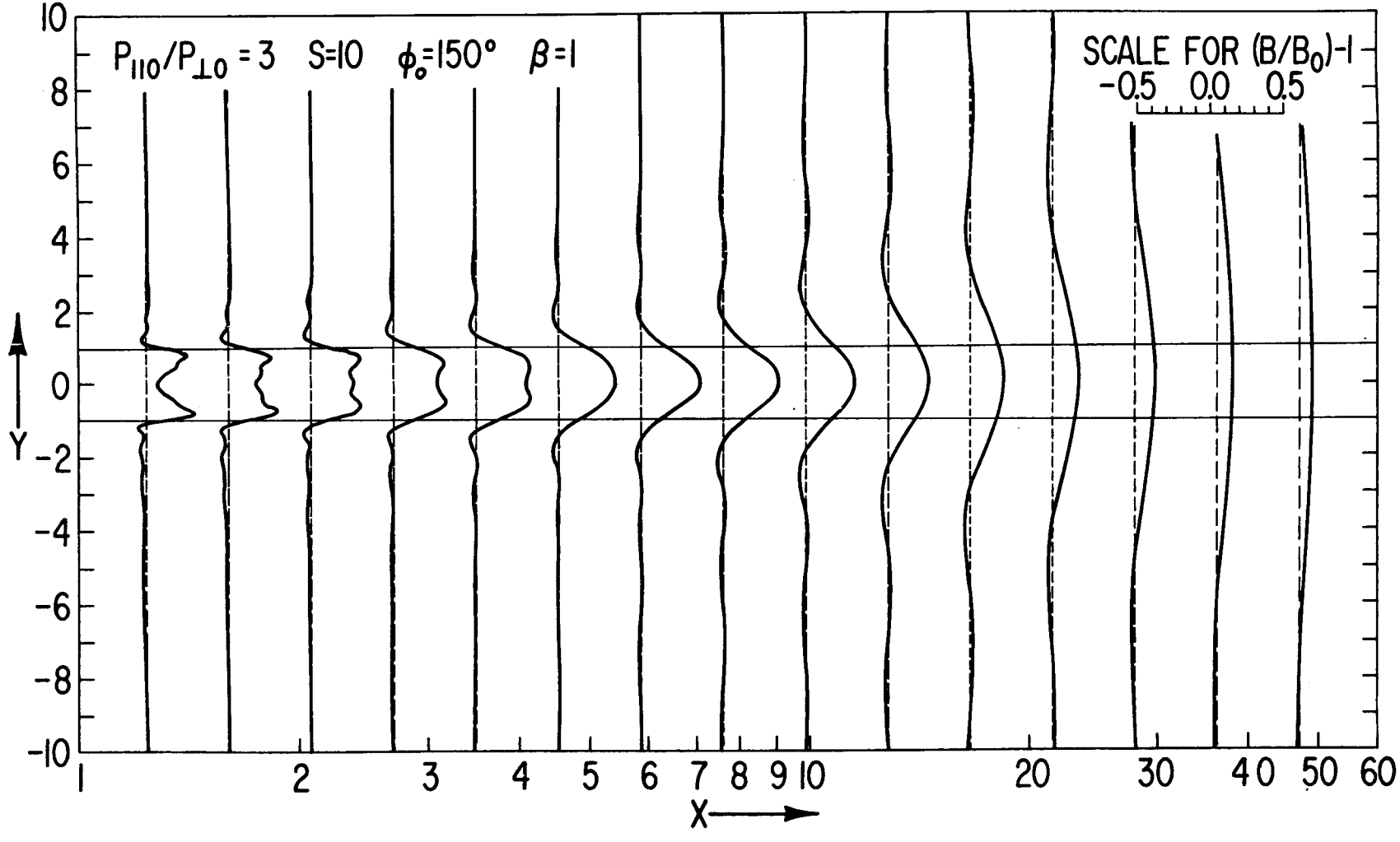
$P_{110}/P_{\perp 0} = 3$ S=10 ϕ_0=150° β=1
SCALE FOR $(B/B_0)-1$
-0.5 0.0 0.5
10
8
6
4
2
0
-2
-4
-6
-8
-10
Y
1 2 3 4 5 6 7 8 9 10 20 30 40 50 60
X

FIG. 4B

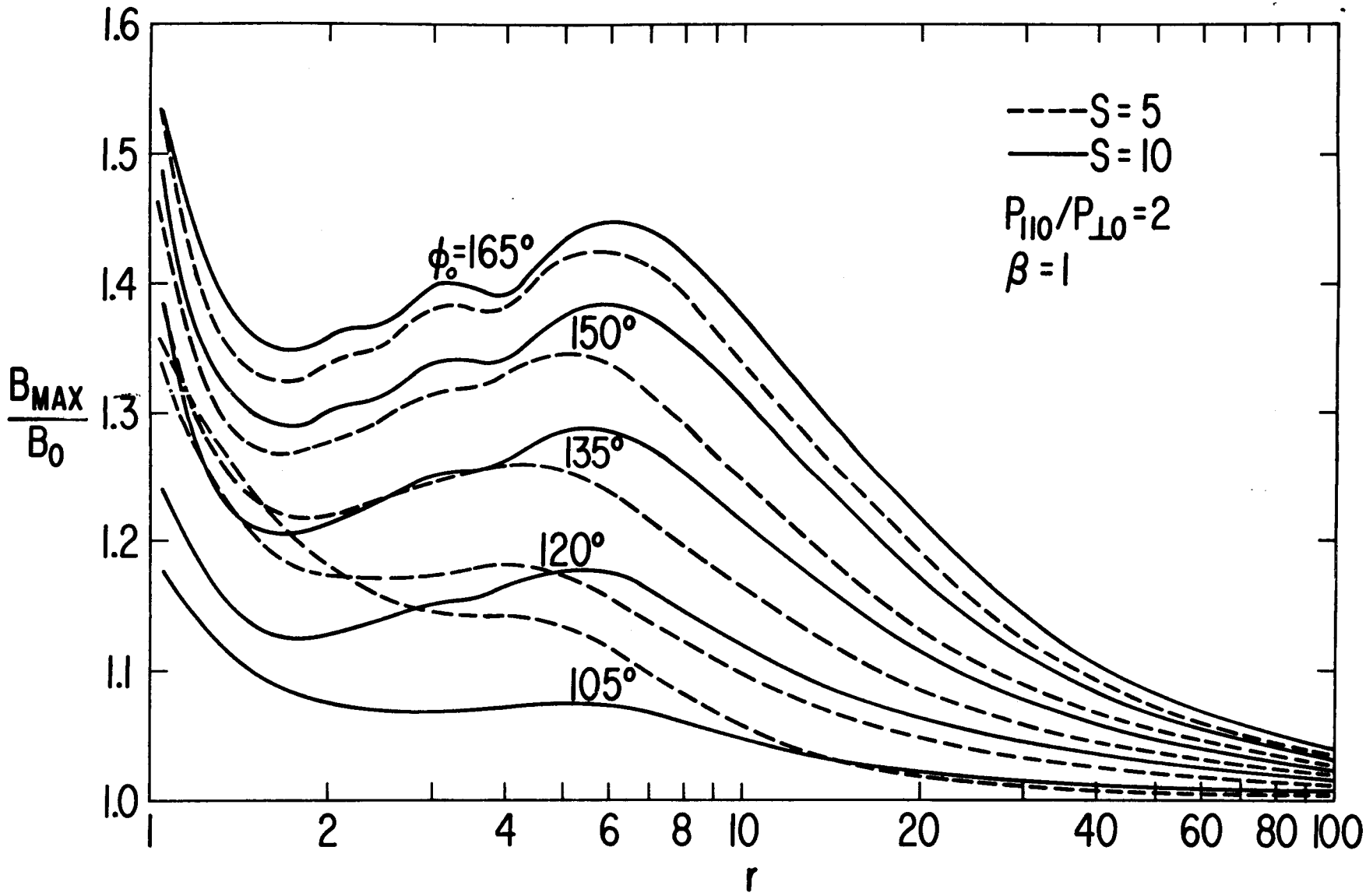
1.6
1.5
1.4
1.3
1.2
1.1
1.0
B_{MAX}/B_0
1
2
4
6
8
10
20
40
60
80
100
r
----S = 5
——S = 10
$P_{110}/P_{\perp 0} = 2$
$\beta = 1$
$\phi_0 = 165°$
150°
135°
120°
105°

FIG. 5